Available online at www.sciencedirect.com
ScienceDirect
Ceramics International 36 (2010) 1719–1723
CERAMICS INTERNATIONAL
www.elsevier.com/locate/ceramint

Short communication

# Effects of variable aspect ratio inclusions on the electrical impedance of an alumina zirconia composite at intermediate temperatures

J.C. Goldsby *

*NASA Glenn Research Center, Cleveland, OH 44135-3191, United States*

Received 12 January 2010; received in revised form 14 January 2010; accepted 4 February 2010
Available online 9 March 2010

**Abstract**

A series of alumina–yttria-stabilized zirconia composites containing either a high aspect ratio (5 and 30 mol%) hexagonal platelet alumina or an alumina low aspect ratio (5 and 30 mol%) spherical particulate was used to determine the effect of the aspect ratio on the temperature-dependent impedance of the composite material. The highest impedance across the temperature range of 373–1073 K is attributed to the grain boundary of the hexagonal platelet second phase in this alumina zirconia composite.
Published by Elsevier Ltd and Techna Group S.r.l.

*Keywords:* B. Composite; Ceramic; AC impedance; Zirconia

## 1. Introduction

Zirconia and its associated alloys are staples among the family of high-temperature technical ceramics. Research remains active in this venerable transition metal oxide system. Current research is application-driven and with each new application a change in properties follows because of the necessary modifications needed to meet the application requirements [1–3]. Recent investigations have focused on incorporating aluminum oxide into yttria-stabilized zirconia to produce an electrolyte with high mechanical toughness, while preserving its electrical characteristics, for applications in solid oxide fuel cells [4,5]. The purpose of this investigation is to elucidate the effects of the second phase aspect ratio with a constant chemical composition on the intermediate temperature-dependent electrical impedance. The two types of secondary phases are a low aspect ratio spherical particulate and a high aspect ratio hexagonal platelet alumina at the same mole percentage.

## 2. Experimental

The samples were received and processed from previous investigations [4]. In summary, from those studies, the raw materials included 10 mol% fully stabilized zirconia powder (Daiichi Kigenso Kagaku Kogyo, Japan) with an average particle size of 4.1 μm, alumina powder 99.99% pure (Baikowski International Corporation, USA) with an average particle size of 0.05 μm, alpha-alumina hexagonal platelet (Elf Atochem, France) with a typical aspect ratio of 10–15 and an average length of 10–15 μm. Samples were processed with standard ceramic processing techniques. The raw materials were hot-pressed in a graphite die at 1500 °C in a vacuum under 30 MPa pressure. The resultant alumina zirconia composite (AZC) compositions included no additions, low aspect and high aspect ratio additions of alumina. The composites are summarized in Table 1. For comparison, a single crystal yttria-stabilized zirconia was also tested. Scanning electron microscopy was performed on all samples after testing. The samples used in this experiment were machined to the following dimensions 2.51 mm × 10 mm × 10 mm. As received samples appeared light to dark gray in color after processing and were consequently, annealed for 1 h at 1100 °C and allowed to cool to room temperature in the furnace. All samples appeared white after annealing.

A standard two-terminal measurement technique was used. Platinum enamel paste was employed as the sample's electrodes, which were specifically designed for ceramic substrates by the Alfa Aesar Chemical Company [6]. The enamel was applied to the surfaces of the test samples, air dried, and heated to 1300 °C for 6 min for curing. Cooled samples

* Tel.: +1 216 433 8250.
*E-mail address:* Jon.C.Goldsby@nasa.gov.

0272-8842/$36.00. Published by Elsevier Ltd and Techna Group S.r.l.
doi:10.1016/j.ceramint.2010.02.016

Table 1
Zirconia alumina composite compositions.

| AZC | 16 | 17 | 20 | 21 | 22 | 25 |
|---|---|---|---|---|---|---|
| mol% alumina spherical particulate | 0 | x | x | 0 | 5 | 30 |
| mol% alumina hexagonal platelet | x | 5 | 30 | x | x | x |

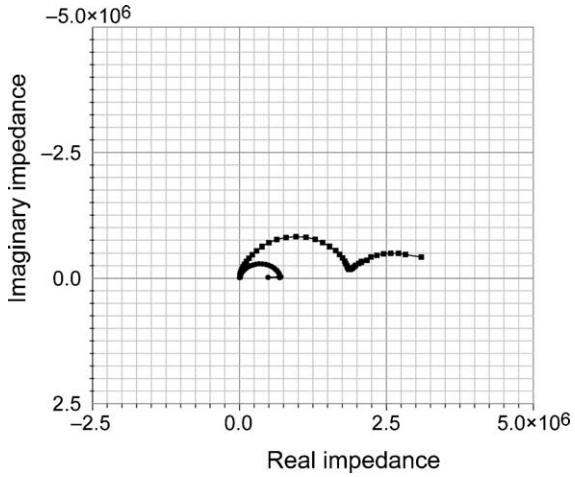


Fig. 1. Impedance spectra for yttria-stabilized zirconia, the two larger arcs are due to the grain and grain boundary of the zirconia polycrystalline matrix (■), The inner arc is from that of a single crystal YSZ (●) taken at 500 K.

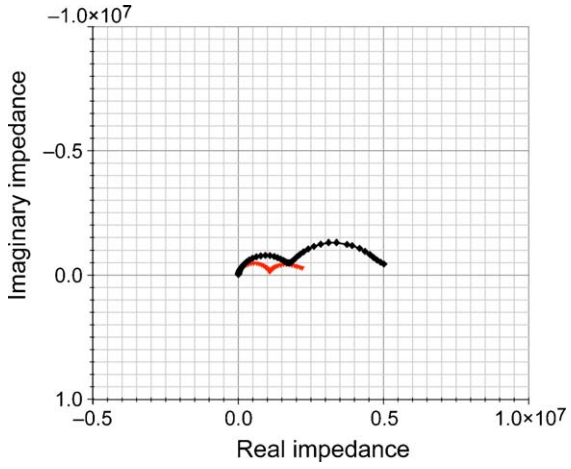


Fig. 2. Impedance spectra for zirconia with 5 (▼) and 30 mol% (◆) low aspect ratio spherical alumina participate composites at 500 K.

were sandwiched between two small platinum foil tabs. The tabs were spot-welded to platinum wire, which provided the external leads for the electrical impedance measurement system. The samples were placed in a spring-loaded clamp fixture, which utilized fused silica rods to support the sample within the hot zone of the furnace. A clamshell furnace with silicon carbide heating elements with a microprocessor-based controller (Eurotherm model 2400) was used to heat and maintain sample temperatures to a precision of greater than 0.1 K. Samples were typically tested from 373 to 1073 K in increments of 10° in air. The frequency was swept from 10 to 1 MHz with an alternating current along with a 0.1 V RMS constant amplitude electric potential. The impedance system utilized in this study was manufactured by Solartron Analytical where a Solartron model 1294 high dielectric interface coupled to an impedance phase gain analyzer Solartron model 1260 was used. The system provided *Impedance* software was used to control the experiment. The entire system was controlled by a National Instruments computer model PXI 8174 with an embedded Intel Celeron 564 MHz processor.

## 3. Results and discussion

Fig. 1 shows a comparison between a single crystal yttria-stabilized zirconia and the yttria-stabilized polycrystalline zirconia matrix material used in this study. It can be clearly seen that the characteristic single semi-circle of the bulk zirconia is visible at this temperature in contrast to the double semi-circle of the polycrystalline which possesses both a grain as well as the grain boundary resistance [7]. In a similar fashion, two semi-circles appear in Fig. 2, an impedance diagram taken at 500 K and is representative of the alumina zirconia composite using two concentrations of spherical particulate alumina at a concentration of 5 and 30 mol%, respectively. Because the second phase inclusion is an insulator no new arcs are generated, only changes in the arc's shape.

This effect becomes pronounced in Fig. 3. The complex impedance diagrams, taken at the same temperature as Fig. 2, indicate the second phase of alumina is the larger aspect ratio hexagonal platelet. The grain boundary arc broadens significantly, indicative of higher real impedance with the higher content of alumina. Composites with the least amount of alumina display a smaller amount of resistance as well as the

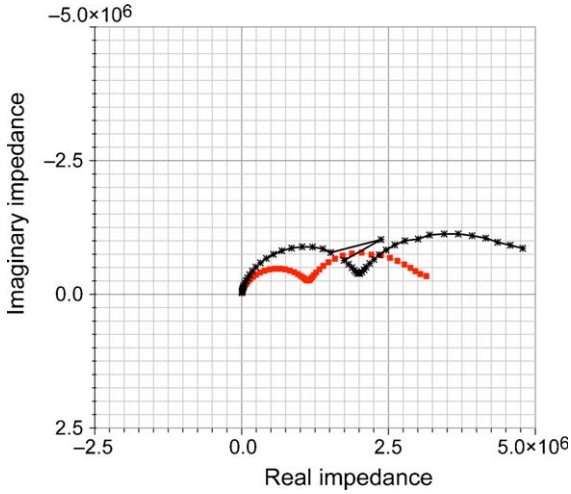


Fig. 3. Impedance spectra for zirconia with 5 (■) and 30 mol% (✱) high aspect ratio hexagonal platelet alumina composites at 500 K.

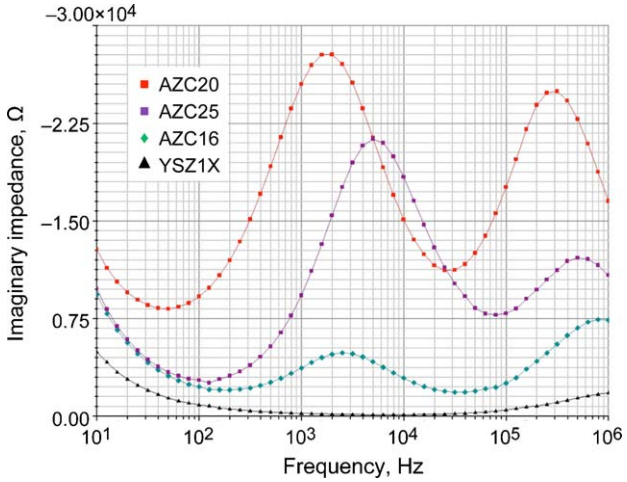


Fig. 4. A comparison of complex imaginary impedance loss for the various compositions; AZC20, AZC25, AZC16, and YSZ1X.

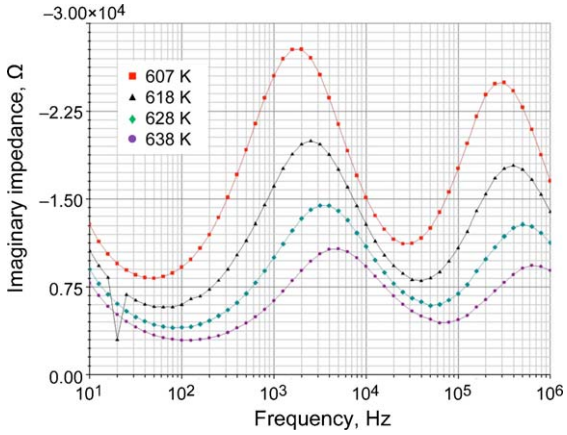


Fig. 5. A comparison of imaginary complex loss with increasing temperature, 607, 618, 628, and 638 K.

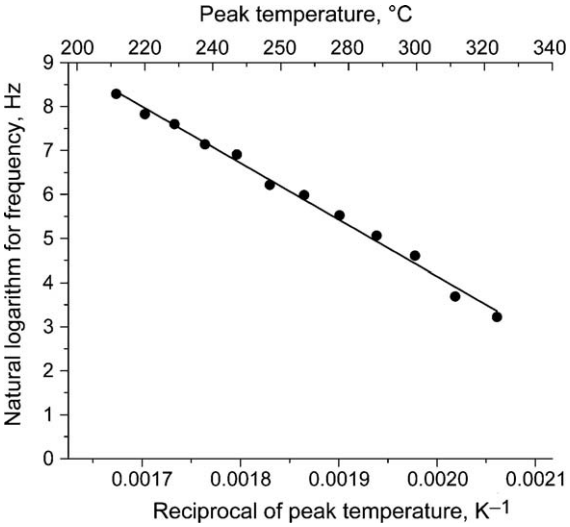


Fig. 6. A linear plot of peak frequency versus temperature used to determine the activation energy.

least amount of impedance loss. However, in comparing the effects of aspect ratio, spherical or low aspect ratio inclusions, yield lower impedance for a given mol% at intermediate temperatures than does the higher aspect ratio inclusions.

In Fig. 4 a comparison is made between a single crystal, a 5 and 30 mol% alumina zirconia composite and either the hexagonal or the spherical particulate addition at 600 K. It appears, based upon the shift in peak heights to higher frequencies with increasing temperature in Fig. 5, that both the intra-grain and grain boundary vacancy motions are thermally activated. Fig. 5 illustrates the 30 mol% alumina hexagonal platelet composite, as seen at various temperatures from 600 up to 638 K in 10 K increments, where the loss decreases with increasing temperature. By utilizing the frequencies at which the peaks occur it is possible to determine the activation energy for the various pathways [8].

$$\ln\left(\frac{f_2}{f_1}\right) = \left(\frac{Q}{k}\right) \times \left(\frac{1}{T_1} - \frac{1}{T_2}\right) \quad (1)$$

The response is a function of frequency and temperature assuming a Boltzmann type distribution. As such the activation energy can be determined by plotting the natural logarithm of frequency versus reciprocal absolute temperature. In this form, Eq. (1) gives the activation energy relationship $f_1$ and $f_2$ as the temperature-dependent peak frequency at temperatures $T_1$ and $T_2$, respectively, $Q$ is the thermal activation energy and $k$ is Boltzmann's constant. Fig. 6 is representative of this relationship produced from Eq. (1), where the slope of the straight line is the ratio of the activation energy to the Boltzmann constant. In this case, the yield activation energy is determined to be 1.11 eV. Table 2 gives the activation energy for both the grains as well as grain boundaries determined for each of the composites. The values appear consistent, 1 eV. The similar activation is indicative of good grain-to-grain contact with little to no secondary phases between the grains [9].

Fig. 7 is a comparative plot of the resistivity with the grains as well as the grain boundaries articulated for the 30 mol% platelet and particulate alumina zirconia composite with respect to a single crystal yttria-stabilized zirconia. It is the single crystal yttria which has the lowest resistivity across the temperature range. The highest resistivity is attributed to the grain boundaries of the hexagonal platelet second phase of the alumina zirconia composite. However, the grain boundary

Table 2
Thermal activation energies of grains and grain interfaces for the alumina yttria-stabilized zirconia composites.

| | AZC 16 | AZC 17 | AZC 20 | AZC 21 | AZC 22 | AZC 25 |
|---|---|---|---|---|---|---|
| Grain activation energy (eV) | 1.082 | 1.101 | 1.047 | 1.025 | 1.098 | 1.120 |
| Grain boundary activation energy (eV) | 1.010 | 1.066 | 1.079 | 1.008 | 1.079 | 0.949 |

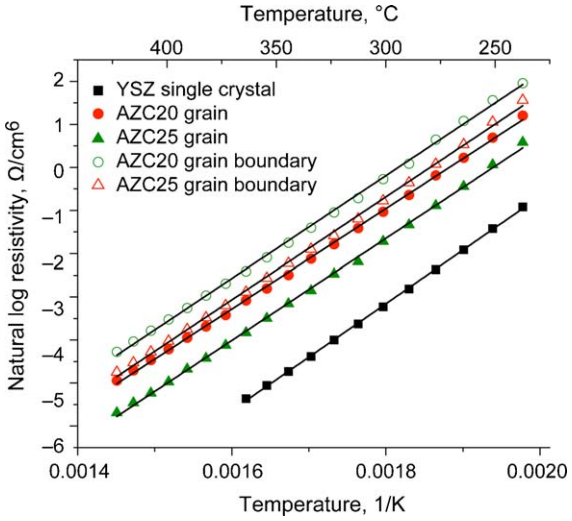


Fig. 7. A comparison of resistivity from the various pathways of the alumina zirconia composites compared with that of a single crystal stabilized zirconia.

resistivity of the spherical particulate alumina zirconia composite appears comparable to the actual grain resistivity of the 30 mol% hexagonal platelet alumina second phase composite.

Fig. 8(a) and (b) are representative microstructures of 30 mol% alumina zirconia composite, for the spherical particulate and hexagonal alumina platelet. The platelet sample contains a much coarser microstructure than that of the spherical particulate sample. Both samples appear to be well-dispersed in the zirconia matrix. In these micrographs, the microstructure is perpendicular to the axis of hot pressing. No large voids are visible with this magnification. The hexagonal alumina–zirconia platelet composites containing oriented-platelet alumina is heavily influenced by the direction of hot pressing. The spherical particulate is of uniform size and distribution throughout its matrix. The inset micrographs in Fig. 8(a) and (b) are of their respective composites under higher magnification along with an energy dispersion spectrograph of the different phases. The platelet sample clearly shows pure alumina inclusions. However, voids appear at some of the triple points, this might occur as a means to accommodate the high aspect ratio second phase. In Fig. 8(b) the low aspect ratio spherical particulate alumina shows a finer microstructure with relatively few pores at the triple points. What is clear from the energy dispersion spectrographic analysis is that the aluminum cations are not dispersed within the zirconia lattice structure, as a substitute for yttrium. Hence the defect chemistry reaction for vacancy conduction remains unchanged. Without the influence of aluminum substituting on the zirconia cation lattice sites, the actual defect clusters are not influenced by the presence of the alumina within the grains. Therefore, the difference in electrical conduction behavior must be attributed to differences in the grain boundary environment from the perspective of the applied electric field.

In postulating a mechanism for temperature-dependent impedance losses one can consider the two phase composite to consist of a series of non-Ohmic junctions, the type of which

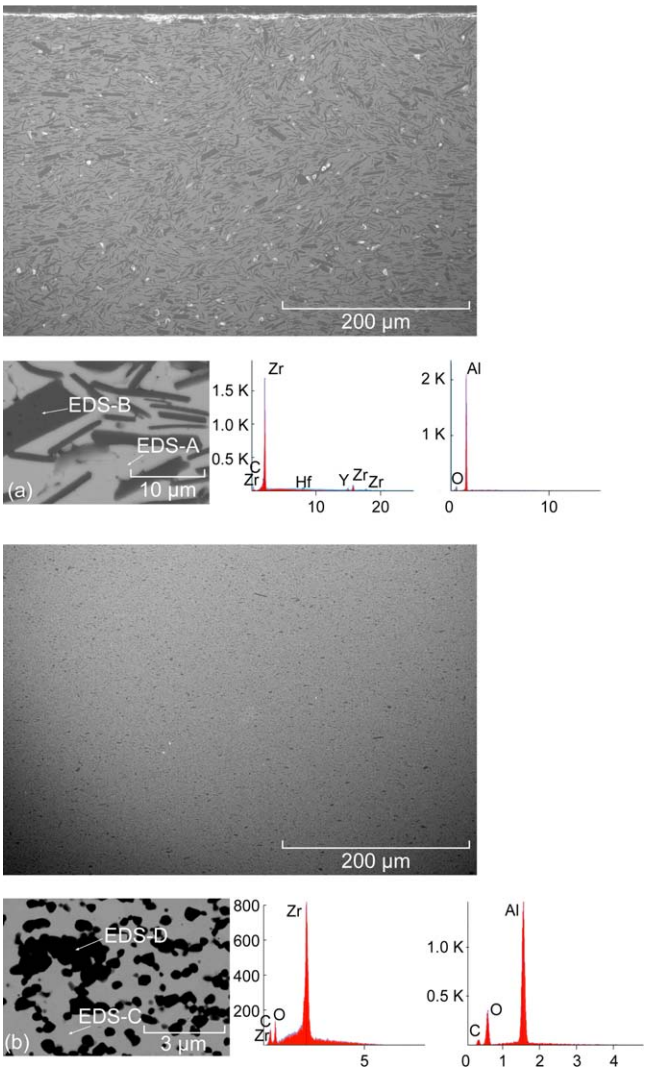


Fig. 8. SEM micrographs of the (a) high aspect ratio alumina reinforcement and (b) low aspect ratio composite with the associated EDS analysis.

being dependent upon the composite's temperature. At low temperatures, the grain-to-grain contact junctions can be considered an insulator-to-insulator type. At intermediate and higher temperatures, oxygen vacancy conduction in the zirconia matrix dominates. Under these conditions zirconia-to-zirconia grain contacts and zirconia to alumina grain contacts can be considered semiconductor-to-semiconductor and semiconductor-to-insulator contacts, respectively. At these junctions, the effect of space charge polarization may influence the vacancy conduction. Given these effects are a surface phenomena, and given hexagonal platelet alumina possesses a higher aspect ratio and subsequently larger surface-to-volume ratios, it must inherently contribute a greater influence on the zirconia grain boundary conduction path than a lower aspect ratio alumina of the same mole percent. In addition, increasing temperature may supply the necessary thermal energy to increase mobility and concentration of charged oxygen vacancies, and consequently, result in the relaxation of space charges and its associated polarization field at the alumina–zirconia boundary.

## 4. Conclusions

In an alumina–yttria-stabilized zirconia composite at intermediate temperatures the aspect ratio of the second phase can contribute to impedance losses. Beyond 600 K the aspect ratio effect decreases, possible as a result of more thermally activated charge carriers and or increased carrier mobility.

## Acknowledgements

This research was funded by the National Aeronautics and Space Administration Subsonic Fixed Wing Program. The author is indebted to Mr. Terry McCue of the Analytical Services Group for his electron microscopy.

## References

[1] L.B. Chen, Surface Review and Letters 13 (2006) 535–544.
[2] A.K. Demin, F.Y. Gulbis, Solid State Ionics 135 (2000) 451–456.
[3] C. Piconi, G. Maccauro, Biomaterials 20 (1999) 1–25.
[4] N.P. Bansal, D.M. Zhu, Ceramics International 31 (2005) 911–916.
[5] S.R. Choi, N.P. Bansal, Ceramics International 31 (2005) 39–46.
[6] J.C. Goldsby, Journal of Alloys and Compounds 321 (2001) 67–71.
[7] R. Brook, Preparation and Electrical Behavior of Zirconia Ceramics, The American Ceramics Society, 1981,, p. 273.
[8] A.S. Nowick, Anelastic Relaxation and Crystalline Solids, Academic press Inc., London, 1972.
[9] N. Bonanos, E. Butler, Applications of Impedance Spectroscopy, John Wiley and Sons Inc., 2005,, p. 205.